2012

Vapor phase polymerization of EDOT from submicrometer scale oxidant patterned by dip-pen nanolithography

Cathal D. O'Connell
University of Wollongong, coc531@uowmail.edu.au

Michael J. Higgins
University of Wollongong, mhiggins@uow.edu.au

Hiroshi Nakashima
Materials Science Research Laboratory, Japan, hiroshin@uow.edu.au

Simon E. Moulton
University of Wollongong, smoulton@uow.edu.au

Gordon G. Wallace
University of Wollongong, gwallace@uow.edu.au

Vapor phase polymerization of EDOT from submicrometer scale oxidant patterned by dip-pen nanolithography

Abstract

Some of the most exciting recent advances in conducting polymer synthesis have centered around the method of vapor phase polymerization (VPP) of thin films. However, it is not known whether the VPP process can proceed using significantly reduced volumes of oxidant and therefore be implemented as part of nanolithography approach. Here, we present a strategy for submicrometer scale patterning of the conducting polymer poly(3,4-ethylenedioxythiophene) (PEDOT) via in situ VPP. Attolitre (10^{-18} L) volumes of oxidant "ink" are controllably deposited using dip-pen nanolithography (DPN). DPN patterning of the oxidant ink is facilitated by the incorporation of an amphiphilic block copolymer thickener, an additive that also assists with stabilization of the oxidant. When exposed to EDOT monomer in a VPP chamber, each deposited feature localizes the synthesis of conducting PEDOT structures of several micrometers down to 250 nm in width. PEDOT patterns are characterized by atomic force microscopy (AFM), conductive AFM, two probe electrical measurement, and micro-Raman spectroscopy, evidencing in situ vapor phase synthesis of conducting polymer at a scale (picogram) which is much smaller than that previously reported. Although the process of VPP on this scale was achieved, we highlight some of the challenges that need to be overcome to make this approach feasible in an applied setting.

Keywords

patterned, oxidant, scale, submicrometer, dip, edot, nanolithography, polymerization, phase, vapor, pen

Disciplines

Engineering | Physical Sciences and Mathematics

Publication Details

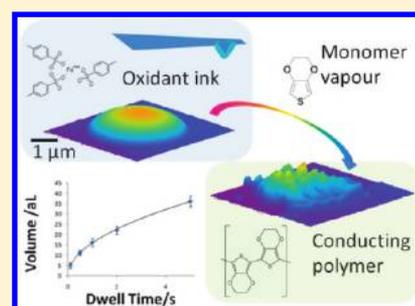# Vapor Phase Polymerization of EDOT from Submicrometer Scale Oxidant Patterned by Dip-Pen Nanolithography

Cathal D. O'Connell,[†] Michael J. Higgins,[†] Hiroshi Nakashima,[‡] Simon E. Moulton,[†] and Gordon G. Wallace[†,*]

[†]ARC Centre of Excellence for Electromaterials Science, Intelligent Polymer Research Institute, AIIM Facility, Innovation Campus, University of Wollongong, Wollongong, NSW 2522, Australia

[‡]Materials Science Research Laboratory, NTT Basic Research Laboratories, NTT Corporation, 3-1, Morinosato Wakamiya, Atsugi, Kanagawa 243-0198, Japan

ⓢ *Supporting Information*

ABSTRACT: Some of the most exciting recent advances in conducting polymer synthesis have centered around the method of vapor phase polymerization (VPP) of thin films. However, it is not known whether the VPP process can proceed using significantly reduced volumes of oxidant and therefore be implemented as part of nanolithography approach. Here, we present a strategy for submicrometer scale patterning of the conducting polymer poly(3,4-ethylenedioxythiophene) (PEDOT) via in situ VPP. Attolitre (10^{-18} L) volumes of oxidant "ink" are controllably deposited using dip-pen nanolithography (DPN). DPN patterning of the oxidant ink is facilitated by the incorporation of an amphiphilic block copolymer thickener, an additive that also assists with stabilization of the oxidant. When exposed to EDOT monomer in a VPP chamber, each deposited feature localizes the synthesis of conducting PEDOT

structures of several micrometers down to 250 nm in width. PEDOT patterns are characterized by atomic force microscopy (AFM), conductive AFM, two probe electrical measurement, and micro-Raman spectroscopy, evidencing in situ vapor phase synthesis of conducting polymer at a scale (picogram) which is much smaller than that previously reported. Although the process of VPP on this scale was achieved, we highlight some of the challenges that need to be overcome to make this approach feasible in an applied setting.

◼ INTRODUCTION

At the core of several emerging fields, including flexible electronics[1] and organic bioelectronics,[2] is the rapid development of organic conductors. Organic conducting polymers (CPs) possess a combination of physical and chemical properties which make them unique electronic conductors,[3] including their soft structure, flexibility, transparency, and tunable functionality. The manufacture of complex devices requires the manipulation of electromaterials into predesigned architectures. Recent advances, such as particles-replication in solvent-resistant templating[4] and advanced inkjet methods exploiting wetting/dewetting strategies,[5,6] have demonstrated the patterning of conducting polymers at resolutions approaching the nanoscale. These innovations highlight the burgeoning potential for cost-effective organic electronic devices.

One of the most intensely studied CPs is currently poly(3,4-ethylenedioxythiophene) (PEDOT) due to its stability over a large pH range, high conductivity, and interesting optoelectronic properties.[7] Much of the most exciting recent progress in PEDOT synthesis has centered around the in situ vapor phase polymerization approach.[8–12] VPP is a relatively rapid and simple method for producing homogeneous CP layers and the highest conductivities for PEDOT generated via the VPP method (currently >1500 S/cm) are generally higher than those reported for other forms of PEDOT, such as PEDOT:polystyrenesulfonate (PEDOT:PSS), even after solvent annealing.[13] Most of the PEDOT VPP studies to date have been thin-film studies where an oxidant solution is first spin-coated onto a substrate before being introduced to the VPP chamber. If the attractive properties of PEDOT formed by VPP are to be fully exploited, however, technologies for the high-resolution patterning of the polymer must be developed.

One patterning strategy is the VPP of PEDOT in predesignated oxidant patterns. In particular, an in situ VPP approach has been demonstrated using inkjet printing as it is highly amenable to patterning liquid-based materials and substances.[14,15] However, the in situ synthesis of CPs by VPP at scales below 10 μm has not been demonstrated. Challenges in scaling down the deposition of liquids to submicron- and nano-scales still remain as many liquid dispensing techniques (e.g., extrusion printing, inkjet printing, microcontact printing, and microplotting) operate within the limit of micrometer resolution. One avenue to address this challenge has been the use of atomic force microscope (AFM) based probe designs with integrated reservoirs and channels to dispense subpicolitre

volumes of liquid.[16,17] The ink used consists of a carrier solvent to assist in the transport of a particulate material, and together they deposit onto the substrate via physioadsorption processes. This AFM-based ink deposition process is generally referred to as dip pen nanolithography (DPN)[18] and enables patterning of a wide range of materials ("inks") including small organic molecules,[19] biomolecules,[20] metal nanoparticles,[21,22] and conducting polymers.[23−25] Its range of feature size resolution (from tens of nanometers up to several micrometers), ability to simultaneously pattern multiple inks,[26] upscalability,[27] and versatility in nondestructive lithography on substrates including semiconductors, plastics, biomaterials, and even biological tissue,[28] mean DPN is a promising tool for the nanostructuring of future nanoelectronic devices.

DPN of conducting polymers has been achieved by several methods, including electrostatically driven transport,[23] in situ polymerization[24] and direct writing of soluble CP.[25] In the interest of developing a complementary high-resolution printing method which may take advantage of the attractive properties of conducting polymer synthesized by VPP, we report on the development of an oxidant ink which is optimized for deposition and patterning via DPN. In addition to the ability to pattern the oxidant on submicrometer length scales, the use of DPN to deposit attolitre volumes of the oxidant ink enables us to explore the feasibility of the VPP of conducting polymer (PEDOT) at significantly reduced dimensions.

■ EXPERIMENTAL SECTION

Materials. The amphiphilic block copolymer poly(ethylene glycol)-*ran*-poly(propylene glycol) MW 12,000 (hereafter PEG−PPG), and 3,4-ethylenedioxythiophene (EDOT) monomer (97%) were obtained from Sigma-Aldrich. Baytron C−B 40 (40 wt % iron(III) *p*-toluenesulfonate in butanol) was obtained from H. C. Stark. All reagents were used without further purification.

Substrate Preparation. Silicon oxide and gold substrates were cleaned by water bath sonication for 10 min each in methanol, acetone, and Milli-Q water. Substrates were cleaned by O_2 plasma (Harrick) for 10 min at 1000 mTorr immediately prior to patterning. Gold substrates were fabricated by depositing gold/chromium (30 nm/10 nm) on glass or silicon wafer using a laboratory-built metal evaporator.

Patterning Methodology. DPN patterning was performed using an Nscriptor system (NanoInk, Skokie, IL) in an environment controlled at 60% relative humidity and 25 °C temperature. The oxidant ink (formulation discussed in results section) was wetted onto a single tip (hereafter "DPN-tip") of NanoInk M-Type probes (NanoInk part no. PEN-0300−03, material Si_3N_4, length 107 μm, width 22 μm, spring constant 0.6 N/m) by dipping for five seconds into the microwell of a NanoInk Universal Inkwell (part no. IWL-0009−03). The tip was bled of excess ink in a method similar to that previously reported for DPN of liquid inks[21,22] by bringing it in contact with the substrate in several (typically four to five) locations, until deposition of large ~10 μm "bleed-spots" ceased. One further test array (25 dots of 5 s dwell time) was deposited in order to ensure the system entered a regime of reproducible submicrometer-scale patterning. Consistent patterning continued for at least 30 min before ink properties began to be modified due to evaporation of the solvent. All patterns were generated using the InkCAD software (v 2.7.1) provided with the Nscriptor system. Patterned substrates were withdrawn from the DPN system, without delay, for immediate VPP.

Vapor Phase Polymerization. The vapor phase chamber consisted of a large desiccator jar connected to a vacuum pump and placed on a hot plate set at 70 °C.[12] The chamber was saturated in 3,4-ethylenedioxythiophene (EDOT) monomer and held at a humidity of 30% ± 5%. The oxidant-patterned samples were placed on a shelf in the middle the chamber, where the temperature was 30−32 °C, and the vacuum switched on. VPP was allowed to proceed under vacuum

for 20 min. The sample was placed in an oven or on a hot plate at 70 °C for 20 min to anneal the PEDOT patterns (this helps prevent stress fracture or delamination during washing step). The washing step involved a careful 10 min soak in ethanol or deionized water.

Instrumentation. AFM topographic imaging was acquired with Nscriptor AFM system (Pacific Nanotechnology) or Asylum Research MFP−3D AFM system in tapping mode in air at room temperature. Conductive AFM (C-AFM) measurements were performed with the ORCA module of the Asylum system equipped with $PtIr_5$ coated conductive probes (Nanoworld, EFM, spring constant: 2.8 N/m) in contact mode in air at room temperature. Electrical characterization of PEDOT DPN printed microwires was performed using a bipotentio-stat (CH1900B, CH Instruments). Raman spectra were obtained on a Jobin Yvon Horiba HR800 Raman spectrometer with LabSpec software using a wavelength of 632.8 nm and a 300 mm^{-1} grating.

■ RESULTS AND DISCUSSION

Ink Formulation and Patterning. We first discuss the formulation of the oxidant ink for DPN writing and the subsequent calibration of feature size using dwell-time and write-speed parameters, demonstrating attolitre control of deposited volumes. Oxidant formulations incorporating iron-(III) *p*-toluenesulfonate (Fe(III) tosylate) and poly(ethylene glycol)-*ran*-poly(propylene glycol) (PEG−PPG) in butanol have been shown to yield PEDOT thin-films exhibiting very high conductivity.[9−11] The polymerization route has been previously described.[12] Fe(III) tosylate rapidly absorbs water from the atmosphere to form crystals and this crystallization inactivates the oxidant. PEG−PPG is an amphiphilic block copolymer which acts as a stabilizer of the oxidant, slowing the water absorption process. Incorporation of poly(ethylene glycol) into VPP−PEDOT is also reported to increase film conductivity in a structure inducing mechanism.[10] Ink transport in DPN can be facilitated via incorporation of a high-viscosity, high boiling point liquid in the ink.[21,22] The PEG−PPG stabilized Fe(III) tosylate spin-coating solution was therefore a good candidate for developing a DPN writeable ink with the PEG−PPG exhibiting trifunctionality, namely: Fe(III) tosylate stabilization, conductivity enhancement, and ink-thickening.

Ink formulations containing 16 wt % Fe(III) tosylate in butanol with a range of loadings of PEG−PPG (4, 6, 12, and 20 wt %) were investigated for DPN patterning. A previously reported formulation optimized for conductivity of spin-coated thin films[11] (16 wt % Fe(III) tosylate in butanol plus 4 wt % PEG−PPG) was not amenable to efficient patterning by DPN due to water absorption and the formation of oxidant crystals on the DPN-tip. Oxidant crystallization occurred more rapidly at high humidities. At low humidities ink-transfer between tip and substrate was not successful, possibly due to a reduction in the water meniscus between tip and substrate (necessary to facilitate molecular ink transport in classic DPN)[18] or a modification in ink properties due to absorbed water. The necessity for high humidity to effect ink transport and yet low humidity to prevent crystallization represents a challenge to the technique. However, environmental conditions were deter-mined (namely 25 °C at 60% relative humidity) which allowed printing with each of the formulations of 6, 12, and 20 wt % PEG−PPG for the duration of a typical patterning experiment (~30 min) without the onset of crystallization. A compre-hensive table illustrating the range of parameters investigated is included in the supplementary section (Table S1, Supporting Information). The 6 wt % PEG−PPG solution was chosen for continued investigation as its patterning was facile, reprodu-cible, and it was the formulation closest to that previously

Table 1. Contact Angles of the Ink Formulation on Relevant Substrates Obtained by Goniometery[a]

	silicon		glass		gold	
	angle (deg)[b]	angle (deg)[c]	angle (deg)[b]	angle (deg)[c]	angle (deg)[b]	angle (deg)[c]
H_2O	49.1 (3.5)	<5	34.2 (3.0)	<5	86.0 (2.6)	24.5 (3.1)
butanol	12.0 (1.8)	<5	16.9 (3.5)	6.4 (2.0)	<5	<5
ink formulation	15.5 (2.5)	13.9 (2.0)	15.3 (1.5)	16.6 (2.0)	12.9 (1.9)	11.3 (2.2)

[a]Parentheses represent standard deviation. Note: contact angles <5° indicate complete or almost complete wetting. [b]Substrate prepared by bath sonication in methanol and H_2O followed by N_2 blow dry. [c]Substrates prepared as above plus additional treatment with O_2 plasma (5 min, 1100 mTorr).

optimized for high conductivity. The 6 wt % PEG−PPG solution is the formulation used henceforth, unless otherwise stated. Contact angle measurements of this ink formulation on the various substrates employed in this study are shown in Table 1. Liquid properties of the ink formulation are outlined in Table 2.

Table 2. Liquid Properties of the Oxidant Ink and of Its Solvent Component

	density (kg m^{-3})	surface tension (N m^{-1})	viscosity (Pa·s)
butanol	0.8057	0.0254 (0.0003)	0.0026
ink formulation	0.87 (0.02)	0.0263 (0.0002)	0.0134 (0.0002)

Arrays of oxidant dots were generated on silicon oxide by depositing at a range of dwell times (Figure 1). Dot diameters of 1.2−5 μm could be deposited utilizing dwell-time control of feature size. At extremely short dwell-times (0.01−0.1 s) dot size reached a minimum of 1.2 μm. This minimum size is comparable to that reported by other liquid-ink DPN studies.[21] Above 0.1 s, both dot diameter and dot height follow power law relationships with dwell time (Figure 1C). The ink calibration curves quoted here refer to silicon oxide substrates only. We have also calibrated the ink according to deposition volume (Figure 1D), where volume is calculated from dot radius and dot height values by assuming each dot as a spherical cap. Conventional microprinting techniques, such as inkjet printing, measure drop deposition in picolitres (10^{-12} L). Ink droplets deposited by DPN, however, are on the order of a million times less voluminous. We have adopted the attolitre (1 aL = 10^{-18} L = 10^6 nm^3) as a convenient unit. Drop volume exhibits $t^{1/2}$ dependence, suggesting dynamics describable in terms of spontaneous capillarity mechanisms under laminar conditions, although detailed discussion of the mechanism of ink transfer is outside the scope of this study. Modeling of the ink-substrate interactions in a similar system has been performed by others.[16] These dimensions of feature-size control highlight the ability of
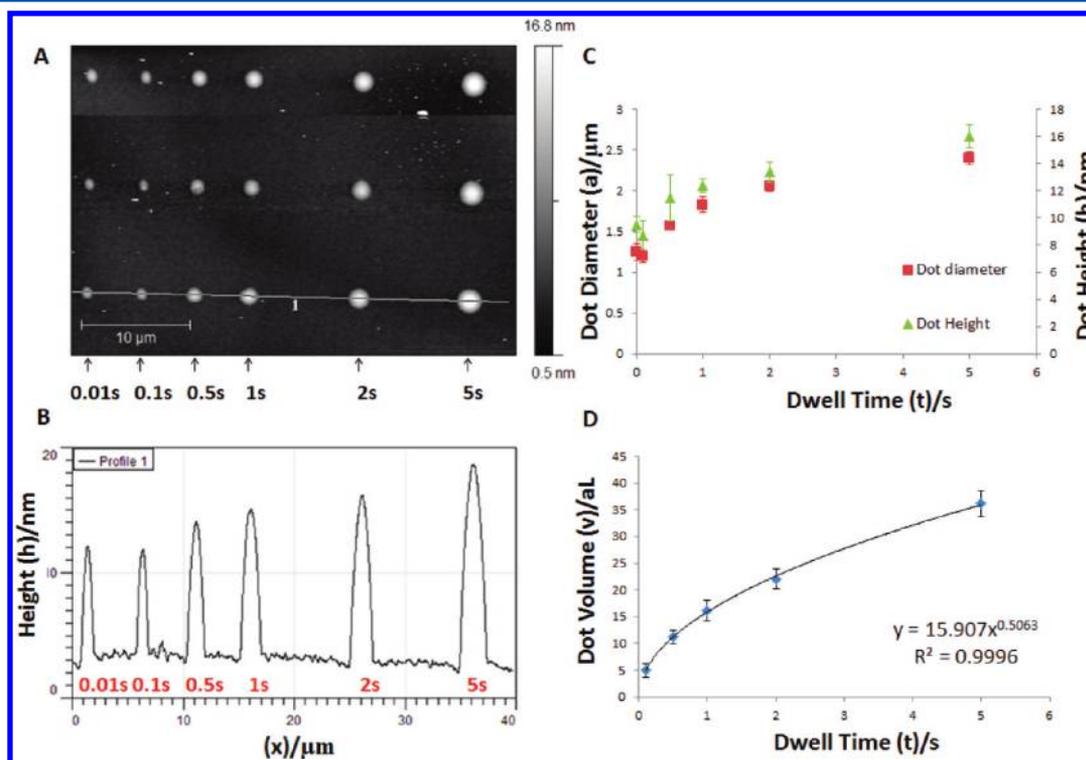

Figure 1. (A) AFM a/c mode topography image of an array of PEDOT dots deposited on silicon with various dwell times. Vertical columns, from left to right, are 0.01, 0.1, 0.5, 1, 2, and 5 s respectively. (B) Topographical data through horizontal line profile in part A. (C) Relationship between dot diameter and dot height with dwell time. Both parameters exhibit power-law dependence with time. (D) Dot volume vs dwell time exhibits $t^{1/2}$ dependence for this dot pattern. Note, the data for 0.01 s dwell time has been omitted from this graph as dot size at very short dwell times is time-independent (see discussion).
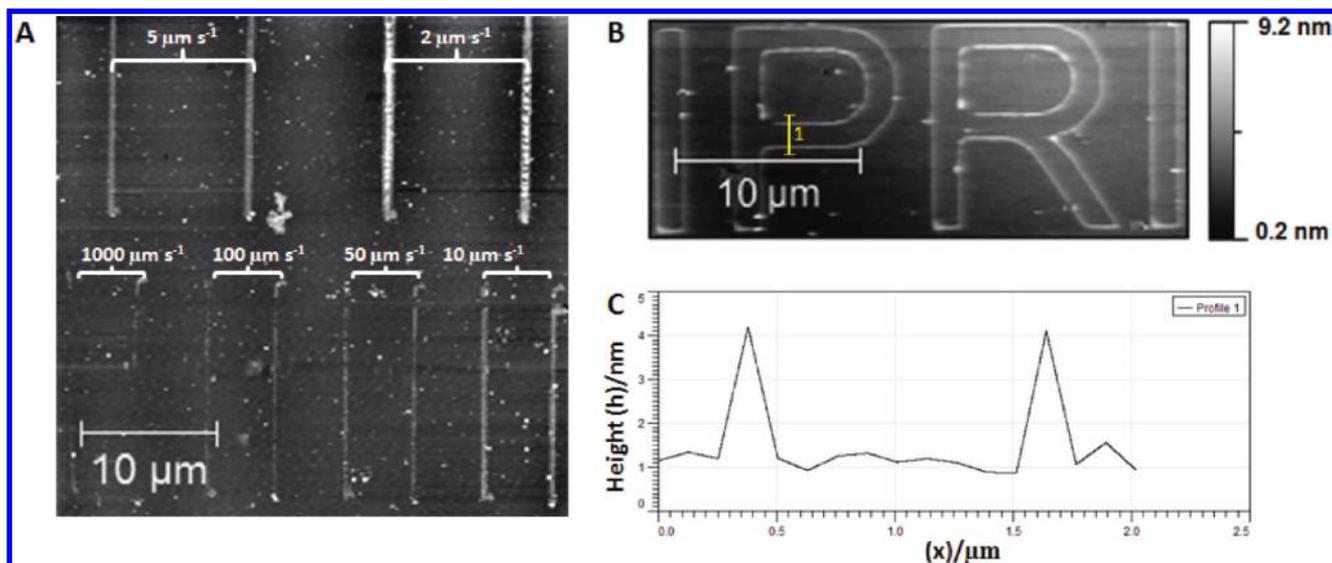
Figure 2. (A) AFM a/c mode phase topography image of oxidant lines (15 μm long) patterned on a Si/SiO$_2$ substrate. The lines drawn at write-speeds of 50 μm s^{-1}, 10 μm s^{-1}, 5 μm s^{-1} and 2 μm s^{-1} correspond to line-widths of 400 nm, 600 nm, 700 and 1000 nm respectively. (B) AFM a/c mode topographical image of an oxidant pattern (IPRI = Intelligent Polymer Research Institute) on Si/SiO$_2$ patterned at a line speed of 10 μm s^{-1}. (C) Topographical data through vertical line profile in (B). Line heights are 4−5 nm and line widths are 250−300 nm.
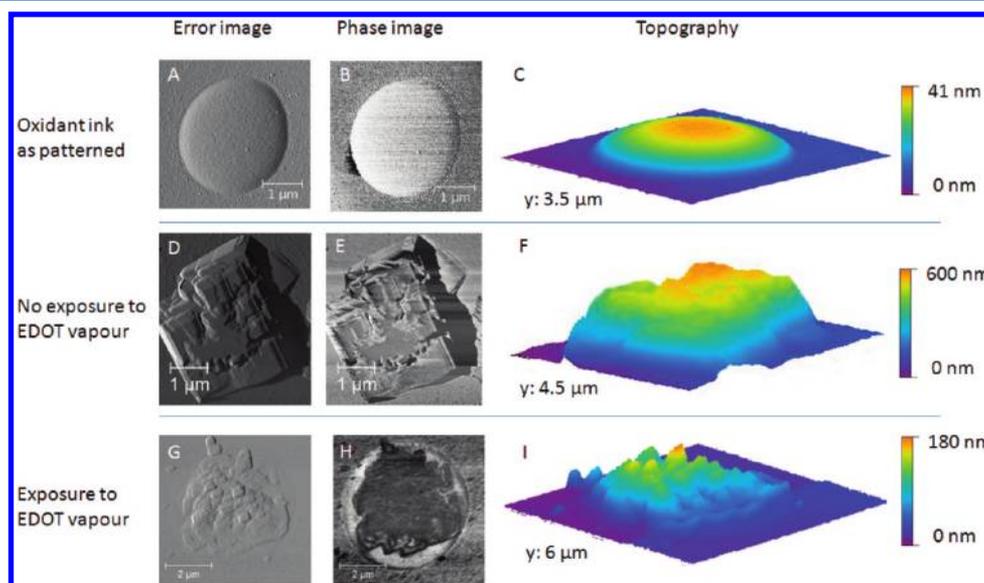

Figure 3. Morphological evidence of PEDOT polymerization from three representative dots after differing treatments: (A) Error image, (B) phase image, and (C) topographical image of a single dot of oxidant ink imaged within 1 h of patterning. The oxidant molecules are stabilized within a matrix of PEG−PPG and residual butanol yielding the smooth spherical cap shape of the as-printed ink: (D) Error image, (E) phase image, and (F) topographical image of a single dot of oxidant ink which has been heated on a hot plate at 65 °C for several minutes without undergoing the VPP step. Heating removes the residual butanol and disrupts the PEG−PPG stabilization effect. The hygroscopic oxidant subsequently absorbs water from the atmosphere to form crystals of several hundred nanometer height: (G) Error image, (H) phase image, and (I) topographical image of a single dot of oxidant ink which has been exposed to EDOT monomer in the vapor phase polymerization chamber prior to heating at 65 °C for several minutes. In this case no crystallization is observed as the oxidant has participated in the EDOT polymerization reaction and then become incorporated in the resulting PEDOT as dopant. The oxidant molecules are thus not liable to water absorption. The morphology of the VPP dot is nodular, contrasting with the smooth as-patterned dot (A−C) and the crystallized non-VPP dot (D−F) above. The phase image (H) reveals the outline of as-patterned ink upon which this polymerization is localized.

DPN, not only to pattern at high resolution, but also to precisely deliver attolitre volumes of liquid reagent.

Line writing was also performed by laterally moving an inked tip while in contact with the substrate (Figure 2). At high write-speeds (>50 μm s^{-1}) discontinuous lines are deposited, while at slower write speeds the lines are continuous and control of line width is afforded by the write speed parameter. As can be seen

in Figure 2B, line writing can achieve considerably improved resolution over dot-deposition. Line-widths of 250−300 nm could be achieved, whereas the minimum dot diameter was 1.2 μm. The difference in achievable feature size may be related to the differing deposition mechanisms. Studies which have examined the capillary forces at play during liquid ink nanodispensing suggest that the dot-deposition event occurs,
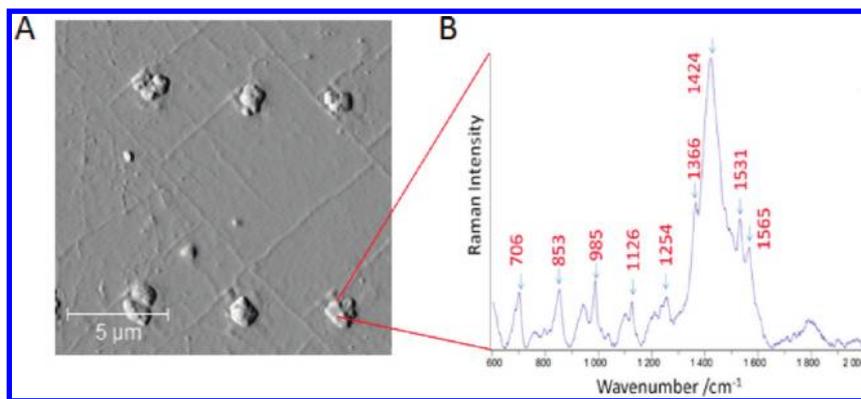
Figure 4. (A) AFM A/C mode error signal image of 6 DPN deposited PEDOT dots after VPP. (B) Typical Raman spectrograph obtained from the PEDOT dot at the bottom left of part A. Characteristic peaks for PEDOT include the C−S−C deflection at 706 cm^{-1}, the oxyethylene ring deformation at 985 cm^{-1}, the C$_\alpha$−C$_{\alpha'}$ (inter ring) stretch at 1254, the C$_\beta$−C$_\beta$ stretch at 1366 cm^{-1}, the symmetric C$_\alpha$=C$_\beta$(−O) stretch at 1424 cm^{-1}, and the asymmetric C$_\alpha$=C$_\beta$ stretch at 1531 cm^{-1}.

not when the tip first contacts the surface, but when it retracts (i.e., as the tip retracts, it distends a "meniscus bridge" of ink between itself and the surface; it the breaking of this meniscus that effects deposition).[16] In line writing, on the other hand, deposition does occur during tip−substrate contact. In this case it is capillary forces that pull ink from the moving tip to the substrate. As such, writing of continuous lines requires extremely fine adjustment of the write-speed to balance the ink−substrate adhesion and ink−ink cohesion forces during writing.

Although line-writing can achieve higher resolution than dot-deposition, line writing is more problematic in practice. The line-width/write-speed relationship is generally less reproducible than dot-width/dwell-time relationship between experiments. Thus, it is difficult to generate line features of a precalculated resolution. For this reason we do not include line-width/write-speed calibration curves as would correspond to Figure 1C. It may be that line-writing is more sensitive to the precise volume of ink in the cantilever reservoir and that the corresponding variations in Laplace pressure may alter the conditions of deposition via capillary action. Achieving line continuity over >10 μm line-length is also difficult. The problem of writing continuous lines of liquid at the submicron-to nano-scale is a very complex one, involving a delicate balance between the forces of liquid cohesion and substrate adhesion. Nanoscale variations in surface energy and nanometer scale roughness variations as well as surface defects can all contribute to a line's continuity. Furthermore, the writing process is all taking place at characteristic liquid thicknesses of a few tens of nanometers or less, well within the regime where dispersive forces tend to dominate and for which contact angles are not well-defined. The quality of patterned lines was also found to vary between different substrates. Gold substrates resulted in more continuous lines compared to SiO$_2$, possibly due to a slightly greater ink−substrate adhesion as evidenced by contact angle studies (see Table 1). Despite this variability in line deposition rate, lines could be patterned across interfaces of gold and silicon dioxide (see Electrical Conductivity).

The prospect of drawing nanometer scale features of liquid ink using a moving pen in contact with the surface is a fascinating opportunity, but further work is needed in this area to fully understand and control the mechanism of deposition by capillary action.

Vapor phase polymerization. The following sections present characterization of oxidant patterns after VPP (now PEDOT), discussing morphology, Raman spectroscopy and electrical characteristics. The morphology of oxidant dots at different stages of the VPP process was compared using AFM a/c mode imaging (Figure 3). The as patterned oxidant dot, imaged 1 h after patterning, exhibits a spherical cap shape with no obvious evidence of Fe(III) tosylate crystallization (Figure 3A−C). This smooth morphology indicates that the incorporation of 6 wt % PEG−PPG is sufficient to stabilize the oxidant against water absorption when kept at room temperature for 1 h. A dot of oxidant ink which has been heated on a hot plate at 65 °C before imaging, however, is completely crystallized (Figure 3D−F). The evaporation of residual butanol from the dot exposes the hygroscopic Fe(III) tosylate which, on cooling, absorbs water from the atmosphere to form large (400−600 nm high) crystals.[11] A dot of oxidant ink which has been exposed to EDOT monomer in the VPP chamber (Figure 3G−I) exhibits a nodular morphology and little, if any, crystallization. In this case the oxidant has polymerized the monomer and the tosylate anion has become incorporated in the resulting PEDOT as dopant.

The post polymerization washing step resulted in a decrease of feature volume to about 13% of the original (see Figure S1, Supporting Information). Dramatic shrinking of VPP−PEDOT thickness postwashing occurs due to the removal of Fe(II) and excess counterion. Previous groups synthesizing VPP−PEDOT (without using PEG−PPG as stabilizer) have reported a shrinkage to 5% of the original volume, and the washing step has even been used as a method to entrap active molecules into the CP matrix.[35] The assertion that all spent oxidant is washed out is supported by several studies which used XPS evidence to conclude that simple methanol or ethanol washing steps were sufficient to remove all traces of Fe(II) from similar VPP−PEDOT systems.[9,34,35] The removal of PEG−PPG is also likely, although a recent study has used XPS and other evidence to suggest the incorporation of a PEG−PPG copolymer into the VPP−PEDOT matrix itself.[35] A theoretical value for the volume reduction can be estimated using the assumptions that 2.5 mol iron(III)tosylate is used to oxidize 1 mol EDOT, that 0.3 mol tosylate remains as dopant in the VPP:PEDOT after washing, that the mass ratio of PEG−PPG to iron(III) tosylate is 0.325 (ink formulation 16 wt % Fe(III) tosylate +6 wt % PEG−PPG in butanol), that all solvent is removed prior to
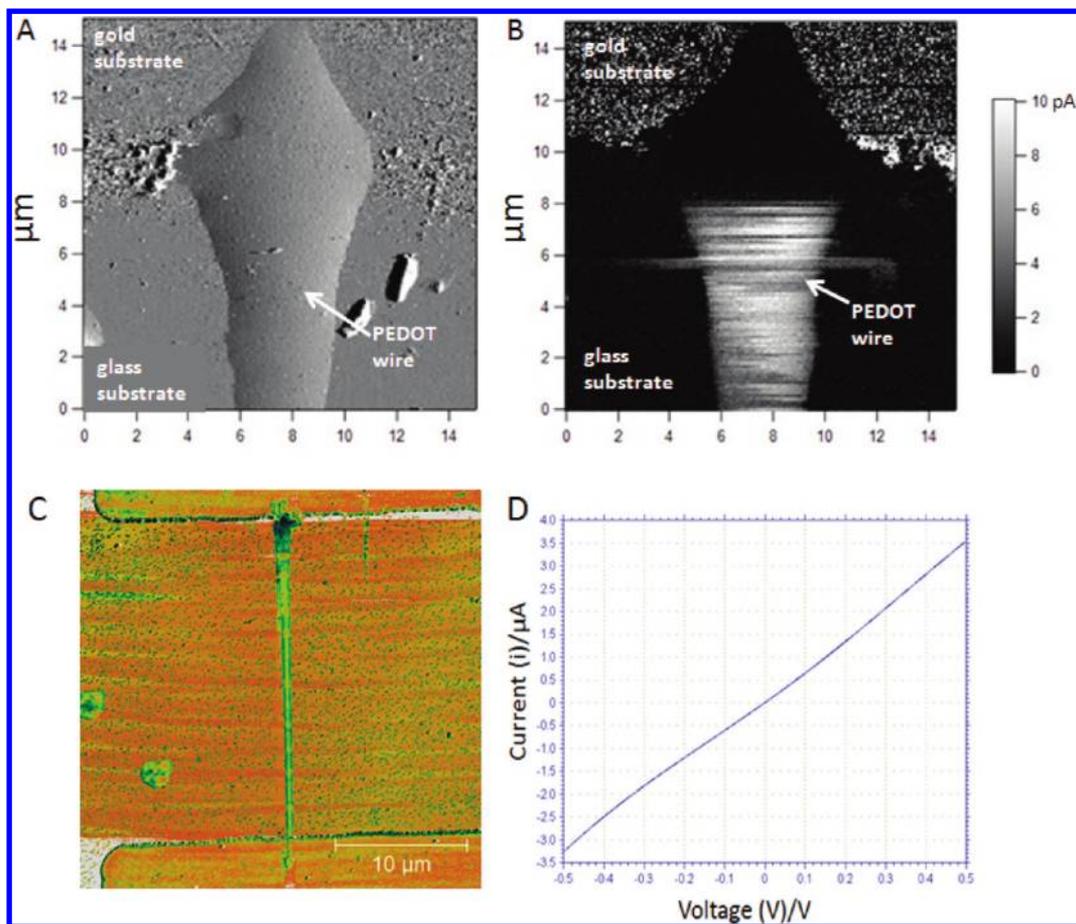
Figure 5. (A) Contact mode deflection image of a line of vapor phase polymerized PEDOT. The patterned line crosses the interface of glass and a 24 nm layer of evaporated gold. (B) Current image at 9 V substrate bias. Light coloring indicates current flow (conducting material), dark coloring indicates no current flow (insulating material). Local current is recorded from the gold substrate but not the glass substrate. Current is measured traveling along the PEDOT wire and across the glass insulator. Note: the inability to measure current in the PEDOT on gold portion is an artifact due to saturation of the current signal by gold on the same (horizontal) scan-line. (C) PEDOT microwire connecting two planar gold electrodes as used for electrical measurements. (D) Current−voltage characteristic of a PEDOT microwire (10 μm width) deposited across a 45 μm insulating gap between planar gold electrodes. The microwire has a resistance of 167 kΩ and a conductivity of 0.7 S cm^{-1}.

VPP, and that the density of the reactants is unity.[36] If all PEG−PPG is washed out, the volume of VPP−PEDOT remaining should be 10% of the original. The reason we see a shrinkage to 13% of the original, and not 10%, may be the result of incorporation of PEG−PPG into the VPP−PEDOT matrix. If this is the case, about 20% of the final VPP−PEDOT volume is composed of PEG−PPG.

Raman Spectroscopy. The synthesis of PEDOT during vapor phase polymerization was confirmed by Raman spectroscopy of a single 2 μm dot (Figure 4). The Raman spectrum exhibits the characteristic peaks of PEDOT,[29] including the C−S−C deflection at 706 cm^{-1}, the oxyethylene ring deformation at 985 cm^{-1}, the $C_\alpha−C_{\alpha'}$ (inter ring) stretch at 1254, the $C_\beta−C_\beta$ stretch at 1366 cm^{-1}, the symmetric $C_\alpha{=}C_\beta(−O)$ stretch at 1424 cm^{-1} and the asymmetric $C_\alpha{=}C_\beta$ stretch at 1531 cm^{-1}. The position of the symmetric $C_\alpha{=}C_\beta(−O)$ stretch at 1424 cm^{-1} is indicative of an oxidized PEDOT structure,[30] confirming that the VPP process can initiate PEDOT formation at such small volumes. Calculating from the AFM morphology and known values for the density of vapor phase polymerized PEDOT:tosylate (2.01 g/cm^3), this single dot contains at most 2.5 pg (1 pg =10^{-12} g) of PEDOT. To our knowledge, this represents an in situ vapor phase synthesis of a conducting polymer on the smallest (picogram) scale to date.

Electrical Conductivity. Assessing the conductivity of conducting polymer patterns at submicrometer scales represents a significant technical challenge. Conductive-atomic force microscopy (C-AFM, also known as current-sensing AFM) was used to qualitatively confirm the conductivity of printed PEDOT wires. C-AFM involves placing an electrical bias on the sample and measuring local conductivity via the current passing through a conductive AFM tip.[31, 32] As direct electrical contact between the sample and tip must be maintained, contact mode imaging is used while simultaneously recording topography and current channels. Parts A and B of Figure 5 show a C-AFM image of a PEDOT microwire patterned across a gold-glass substrate interface. A current signal is clearly measured from the gold substrate and from along the PEDOT wire. Measurement of current indicates conductive areas of the scanned surface and confirms the electrical conductivity of the PEDOT microwire. No current is measured from the glass (insulating) substrate.

Higher loading forces can be used to decrease contact resistance and increase stability but in our case a high force had the effect of smearing the PEDOT patterns. The high contact resistance, coupled with the necessity to apply very low loading forces (0.05 nN) necessitated a high surface bias (9 V), although a current signal was measured from PEDOT at

voltages as low as 3 V. The large contact resistance between tip and sample made quantitative measurements prohibitively difficult for this system.

Quantitative electrical conductivity measurements were performed by measuring the current−voltage characteristics of PEDOT microwires bridging an insulating gap (25 or 45 μm) between planar electrodes (Figure 5, parts C and D). Larger microwires (∼10 μm width) were used for ease of measurement. Measurements were undertaken on unwashed samples as the washing step had the effect of breaking microwire connectivity. Conductivity of these microwires was calculated to be 1 ± 0.5 S cm^{-1}. This value, while being comparable to that of commercially available PEDOT:poly-(styrene sulfate) dispersions previously patterned by DPN,[25] is still far below the highest reported conductivity values of PEDOT thin films synthesized by VPP. The measured conductivity of a conducting polymer sample can vary significantly depending on the particular system geometry, and depending upon subtleties of the measurement per-formed.[33] Therefore, the direct comparison of PEDOT microwire conductivity with that of the equivalent spin-coated thin film probably has limited meaning. Nevertheless, we suggest three possible reasons for the discrepancy between our VPP−PEDOT microwire properties and that of the literature record spin-coated VPP−PEDOT: (1) The strongest effect is most likely the large volume percentage of spent oxidant which must persist in the unwashed microwires. The disruptive effect of the washing step on microwire connectivity highlights the increased difficulty of achieving adequate adhesion at reduced scales (thin films submitted to the same treatment exhibit no observable delamination). We are currently investigating methods, such as the utilization of adhesion promoting substrate treatements, which may effect covalent attachment of the VPP−PEDOT to the substrate. (2) The contact resistance of the microwire-Au contacts is likely very high, due to the tiny area of contact (∼5 μm^2) and the weak, physioadsorbed nature of the connection. This extra resistance is included twice-over in the measured resistance value and its subtraction would result in a more realistic, and certainly higher, conductivity value for the PEDOT microwire. (3) Vapor phase chamber conditions were a factor. The optimization of the vapor phase parameters were outside the scope of this study and hence humidity, temperature, and pressure were not precisely controlled. In our laboratory, the PEDOT thin-films generated from spin-coated films of our ink formulation had conductivities of ∼100 S cm^{-1}, already an order of magnitude lower than some literature values. No doubt significant improvements in microwire conductivities would follow a more directed optimization of vapor phase conditions.

■ CONCLUSION

To our knowledge, this is the first demonstration of patterning conducting polymer by DPN via VPP. Furthermore, the use of DPN allowed us to demonstrate that the in situ polymerization of a conducting polymer by the vapor phase could proceed within attolitre volumes of an oxidant ink. As proof of concept, we have confirmed the polymerization of picogram scale individual PEDOT features by Raman spectroscopy and confirmed the conductivity of patterned PEDOT microwires. Although this concept aims to take advantage of the VPP process, we have shown that further optimization (e.g., ink properties, conductivity) at the nanoscale are required. The downscaling of the VPP process toward a micrometer to submicrometer scale presents new challenges not encountered in thin film studies, in particular: (1) the relatively increased rate of water induced crystallization due to the greater surface area to volume ratio, (2) the change of ink properties over time due to solvent evaporation from the cantilever, and (3) the challenge of effecting strong adhesion between the VPP−PEDOT pattern and the substrate. We have found that challenge 1 could be overcome by increasing the PEG−PPG content of the ink. The utilization of a solvent carrier system with lower vapor pressure may alleviate the curtailing of patterning time due to change in ink properties with time. In addition, functionalization of the surface with adhesion promoters such as γ-glycidoxypropyltrimethoxysilane may improve the stability of microwires during the washing step. With a greater fundamental understanding of the ink deposition, VPP process (e.g., diffusion and nucleation kinetics of monomer) and suitable means for quantifying the conductive properties of nanoelectromaterials, the controlled deposition of attolitre volumes of liquid reagent has potential to introduce a unique strategy for in situ synthesis of predefined architectures.

■ ASSOCIATED CONTENT

Ⓢ Supporting Information

Table showing a selection of patterning parameters inves-tigated, including PEG content, percent relative humidity, substrate temperature, substrate type. 3D image rendered from optical profilometry of an array of VPP−PEDOT features before and after H$_2$O washing step. This material is available free of charge via the Internet at http://pubs.acs.org/.

■ AUTHOR INFORMATION

Corresponding Author

*E-mail: gwallace@uow.edu.au.

Notes

The authors declare no competing financial interest.

■ ACKNOWLEDGMENTS

■ REFERENCES

(1) Forrest, S. R. The path to ubiquitous and low-cost organic electronic appliances on plastic. *Nature* **2004**, 911−918.

(2) Pron, A.; Gawrys, P.; Zagorska, M.; Djurado, D.; Demadrille, R. Electroactive materials for organic electronics: preparation strategies, structural aspects and characterization techniques. *Chem. Soc. Rev.* **2010**, *39*, 2577−2632.

(3) Wallace, G. G.; Spinks, G. M. *Conductive Electroactive Polymers*; CRC Press: Boca Raton, FL, 2008.

(4) Mele, E.; Camposeo, A.; De Giorgi, M.; Di Benedetto, F.; De Marco, C.; Tasco, V.; Cingolani, R.; Pisignano, D. Sub-50-nm conjugated polymer dots by nanoprinting. *Small* **2008**, *4*, 1894−9.

(5) Sirringhaus, H.; Kawase, T.; Friend, R. H.; Shimoda, T.; Inbasekaran, M.; Wu, W.; Woo, E. P. High-Resolution Inkjet Printing of All-Polymer Transistor Circuits. *Science* **2000**, *290*, 2123−2126.

(6) Wang, J. Z.; Zheng, Z. H.; Li, H. W.; Huck, W. T. S.; Sirringhaus, H. Dewetting of conducting polymer inkjet droplets on patterned surfaces. *Nature Mater.* **2004**, *3*, 171−6.

(7) Elschner, A.; Kirchmeyer, S.; Lövenich, W.; Merker, U.; Reuter, K. *PEDOT: Principles and Apllications of an Intrisically Conductive Polymer*; CRC Press: Boca Raton, FL, 2002; p 353.

(8) Winther-Jensen, B.; Winther-Jensen, O.; Forsyth, M.; Macfarlane, D. R. High rates of oxygen reduction over a vapor phase-polymerized PEDOT electrode. *Science* **2008**, *321*, 671−4.

(9) Fabretto, M.; Autere, J.-P.; Hoglinger, D.; Field, S.; Murphy, P. Vacuum vapour phase polymerised poly (3, 4-ethyelendioxythiophene) thin films for use in large-scale electrochromic devices. *Thin Solid Films* **2011**, *519*, 2544−2549.

(10) Winther-jensen, B.; Knecht, T.; Ong, C.; Vongsvivut, J.; Clark, N. Inhomogeneity Effects in Vapor Phase Polymerized PEDOT: A Tool to Influence Conductivity. *Macromol. Mater. Eng.* **2011**, 185−189.

(11) Zuber, K.; Fabretto, M.; Hall, C.; Murphy, P. Improved PEDOT Conductivity via Suppression of Crystallite Formation in Fe(III) Tosylate During Vapor Phase Polymerization. *Macromol. Rapid Commun.* **2008**, *26*, 1503−1508.

(12) Fabretto, M.; Zuber, K.; Hall, C.; Murphy, P. High Conductivity PEDOT Using Humidity Facilitated Vacuum Vapour Phase Polymer-isation. *Macromol. Rapid Commun.* **2008**, 1403−1409.

(13) Kim, Y. H.; Sachse, C.; Machala, M. L.; May, C.; Müller-Meskamp, L.; Leo, K. Highly Conductive PEDOT:PSS Electrode with Optimized Solvent and Thermal Post-Treatment for ITO-Free Organic Solar Cells. *Adv. Funct. Mater.* **2011**, *21*, 1076−1081.

(14) Winther-jensen, B.; Clark, N.; Subramanian, P.; Helmer, R.; Ashraf, S.; Wallace, G. G.; Spiccia, L.; Macfarlane, D. Application of Polypyrrole to Flexible Substrates. *J. Appl. Polym. Sci.* **2007**, *104*, 3938−3947.

(15) Choi, J. S.; Cho, K. Y.; Yim, J.-H. Micro-patterning of vapor-phase polymerized poly (3, 4-ethyenedioxythiophene) (PEDOT) using ink-jet printing/soft lithography. *Eur. Polym. J.* **2010**, *46*, 389−396.

(16) Fang, A.; Dujardin, E.; Ondarçuhu, T. Control of droplet size in liquid nanodispensing. *Nano Lett.* **2006**, *6*, 2368−74.

(17) Hwang, K.; Shin, C.; Mingwu, R.; Lee, S.-H.; Kim, H.-M. Design of a nano-printer based on AFPN (Active Fountain Pen Nano-lithography) using switch control. *J. Mech. Sci. Technol.* **2011**, *25*, 977−985.

(18) Piner, R. D.; Zhu, J.; Xu, F.; Hong, S.; Mirkin, C. A. "Dip-pen" Nanolithography. *Science* **1999**, *283*, 661−663.

(19) Lee, K. B.; Lim, J.-H.; Mirkin, C. A. Protein Nanostructures Formed via Direct-Write Dip-Pen Nanolithography. *J. Am. Chem. Soc.* **2003**, *1*, 5588−5589.

(20) Li, J.; Lu, C.; Maynor, B.; Huang, S.; Liu, J. Controlled Growth of Long GaN Nanowires from Catalyst Patterns Fabricated by "Dip-Pen" Nanolithographic Techniques. *Chem. Mater.* **2004**, *16*, 1633−1636.

(21) Wang, H.-T.; Nafday, O. A.; Haaheim, J. R.; Tevaarwerk, E.; Amro, N. A.; Sanedrin, R. G.; Chang, C. Y.; Ren, F.; Pearton, S. J. Toward conductive traces: Dip Pen Nanolithography of silver nanoparticle-based inks. *Appl. Phys. Lett.* **2008**, 143105.

(22) Hung, S.-C.; Nafday, O. A.; Haaheim, J. R.; Ren, F.; Chi, G. C.; Pearton, S. J. Dip Pen Nanolithography of Conductive Silver Traces. *J. Phys. Chem. C* **2010**, 9672−9677.

(23) Lim, B. J.-hyurk; Mirkin, C. A. Electrostatically Driven Dip-Pen Nanolithography of Conducting Polymers. *Adv. Mater.* **2002**, *14*, 1474−1477.

(24) Su, M.; Aslam, M.; Fu, L.; Wu, N.; Dravid, V. P. Dip-pen nanopatterning of photosensitive conducting polymer using a monomer ink. *Appl. Phys. Lett.* **2004**, *84*, 4200−4202.

(25) Lu, H.-H.; Lin, C.-Y.; Hsiao, T.-C.; Fang, Y.-Y.; Ho, K.-C.; Yang, D.; Lee, C.-K.; Hsu, S.-M.; Lin, C.-W. Electrical properties of single and multiple poly(3,4-ethylenedioxythiophene) nanowires for sensing nitric oxide gas. *Anal. Chim. Acta* **2009**, *640*, 68−74.

(26) Hong, S.; Zhu, J.; Mirkin, C. A. Multiple Ink Nanolithography: Toward a Multiple-Pen Nano-Plotter. *Science* **1999**, *286*, 523−525.

(27) Huo, F.; Zheng, Z.; Zheng, G.; Giam, L. R.; Zhang, H.; Mirkin, C. A. Polymer pen lithography. *Science* **2008**, 1658.

(28) Sistiabudi, B. R.; Ivanisevic, A. Dip-Pen Nanolithography of Bioactive Peptides on Collagen-Terminated Retinal Membrane. *Adv. Mater.* **2008**, 3678−3681.

(29) The AFM error image is generated from the vertical displacement of the laser spot on the AFM photodetector and can be useful for highlighting topographical steps or boundaries. The phase image is generated from the phase lag between the AC input signal (which drives the cantilever) and the photodetector output signal (a function of cantilever resonance). Variations in sample composition and mechanical properties can be highlighted in the phase image.

(30) Cooney, R. P.; Bowmaker, G. A.; Chiu, W. W.; Trava, J. Studies of dopant effects in poly(3,4-ethylenedioxythiophene) using Raman spectroscopy. *J. Raman Spectrosc.* **2006**, 1354−1361.

(31) O'Neil, K. D.; Shaw, B.; Semenikhin, O. On the origin of mesoscopic inhomogeneity of conducting polymers. *J. Phys. Chem. B* **2007**, *111*, 9253−69.

(32) Guo, D.-Z.; Hou, S.-M.; Zhang, G.-M.; Xue, Z.-Q. Conductance fluctuation and degeneracy in nanocontact between a conductive AFM tip and a granular surface under small-load conditions. *Appl. Surf. Sci.* **2006**, *252*, 5149−5157.

(33) Fabretto, M.; Zuber, K.; Jariego-Moncunill, C.; Murphy, P. Measurement Protocols for Reporting PEDOT Thin Film Con-ductivity and Optical Transmission: A Critical Survey. *Macromol. Chem. Phys.* **2011**.

(34) Ali, M. A.; Kim, H.; Lee, C.; Nam, H.; Lee, J. Effects of iron(III) p-toluenesulfonate hexahydrate oxidant on the growth of conductive poly(3,4-ethylenedioxythiophene) (PEDOT) nanofilms by vapor phase polymerization. *Synth. Met.* **2011**, *161*, 1347−1352.

(35) Fabretto, M.; Jariego-Moncunill, C.; Autere, J.-P.; Michelmore, A.; Short, R. D.; Murphy, P. High conductivity PEDOT resulting from glycol/oxidant complex and glycol/polymer intercalation during vacuum vapour phase polymerization. *Polymer* **2011**, *52*, 1725−1730.

(36) Winther-Jensen, B.; Chen, J.; West, K.; Wallace, G. "Stuffed" conducting polymers. *Polymer* **2005**, *46*, 4664−4669.